and hence we take the number of degrees of freedom as 4, obtaining a value $P(\chi^2, 4)$ of 0.67, indicating that the data are consistent with the theoretical relation (1).

Figure 1*b* shows the value of $P(\chi^2, 4)$ plotted as a function of T after χ^2 has been minimised with respect to A, B and C. The best value of T, indicated by the maximum of this curve, is (222 ± 16) K; the error estimate corresponds to one-half the half-width of the P curve at $P = 0.05$. Subsequent measurements during May 1979 indicated substantially lower temperatures, near 170 K, between 90 and 94 km. Small negative corrections can be applied to the measured temperatures after taking into account the finite laser linewidth. If $\Delta\nu_D$ represents the Doppler linewidth of each hyperfine component and $\Delta\nu_L$ is the laser linewidth, it can be shown by replacing equation (1) by its convolution with a gaussian laser line-shape function that the first-order correction is given by

$$\frac{\Delta T}{T} = -(\Delta\nu_L/\Delta\nu_D)^2 \qquad (4)$$

which amounts to less than 3K for our measurements.

It is to be expected that the present method of measuring upper atmosphere temperatures will be capable of greater accuracy than that involving the use of a sodium absorption cell in the receiver which depends on integration over the spectral line shape. The accuracy currently available with the new technique can be substantially improved by the use of high laser repetition rates, improvements in receiver sensitivity and maximum photon counting rates, and optimum choice of laser frequencies. The capability of observing the small-scale structure of temperature offered by this laser technique is directly relevant to studies of the thermal balance of the upper mesosphere, of the neutral and ion chemistry involving temperature dependent rate coefficients, of noctilucent clouds and of short-wavelength atmospheric-wave disturbances. This ground-based technique could, therefore, be a useful supplement to existing satellite measurements of temperature based on observations of thermal emissions.

Received 14 June; accepted 9 August 1979.

1. Sandford, M. C. W. & Gibson, A. J. *J. atmos. terr. Phys.* **32**, 1423–1430 (1970).
2. Schuler, C. J., Pike, C. T. & Miranda, H. A. *Appl. Phys. Lett.* **19**, 345–348 (1971).
3. Hake, R. D. *et al. J. geophys. Res.* **77**, 6839–6848 (1972).
4. Blamont, J. E., Chanin, M. L. & Megie, G. *Ann. Geophys.* **287**–838 (1972).
5. Kirchhoff, V. W. J. H. & Clemesha, B. R. *J. atmos. terr. Phys.* **35**, 1493–1498 (1973).
6. Aruga, T., Kamiyama, H., Jyumonji, M., Kobayasi, T. & Inaba, H. *Rep. Ion. Sp. Res., Jap.* **28**, 65–68 (1974).
7. Rowlett, J. R., Gardner, C. S., Richter, E. S. & Sechrist, C. F. *Geophys. Res. Lett.* **5**, 683–686 (1978).
8. Kusch, P. & Taub, H. *Phys. Rev.* **75**, 1477 (1949).
9. Chamberlain, J. W., Hunten, D. M. & Mack, J. E. *J. atmos. terr. Phys.* **12**, 153–165 (1958).
10. Hänsch, T. W., Shahin, I. S. & Schawlow, A. L. *Phys. Rev. Lett.* **27**, 707–710 (1971).
11. Schuda, F., Hercher, M. & Stroud, C. R. *Appl. Phys. Lett.* **22**, 360–362 (1973).
12. Bhattacharyya, S. K., Gibson, A. J., Hammond, E., Sandford, M. C. W. & Thomas, L. *Opt. Quant. Electron.* **10**, 243–252 (1978).

Environmental fluctuation effects on the global energy balance

C. Nicolis

Institut d'Aéronomie Spatiale de Belgique, 1180 Bruxelles, Belgique

G. Nicolis

Faculté des Sciences de l'Université Libre de Bruxelles, Campus plaine, CP 226, 1050 Bruxelles, Belgique

Much effort has been devoted to developing simple energy-balance climatic models. Although consideration of latitudinal energy transfer[1–4] gives more complete answers it has become clear that global, 'zero dimensional' models may also provide much useful information[5,6]. These models have the form:

$$C\frac{dT}{dt} = Q(1-a(T)) - \varepsilon\sigma T^4 \qquad (1)$$

T is the surface temperature, C the thermal inertia coefficient, Q the solar constants, σ the Stefan constant, $a(T)$ the (generally temperature-dependent) albedo, and ε the emissivity of the Earth–atmosphere system. The variability of the climate system rests, therefore, on certain types of change experienced by the solar output, or by such planetary factors as emissivity, albedo, cloudiness and so forth. In addition to some long-term trends of the solar constant[7], it has been suggested that the Sun is in an almost-intransitive state[8,9]. Hence, it may generate large fluctuations around some mean value of its output, which will be perceived by the Earth–atmosphere system as an 'external noise' affecting Q. The fact that the terrestrial atmosphere is likely to be in an almost intransitive state[10] can also generate appreciable fluctuations in factors influencing the albedo and the emissivity. In the absence of precise knowledge of the mechanism of these fluctuations, one is again tempted to regard them as an 'external noise' affecting $a(T)$ and ε. We explore here the qualitative effect of such environmental fluctuations in the thermal regime[13], at the level of a zero-dimensional planetary model. Previous analyses of nonlinear systems of chemical and biological interest[11,12] have shown that external noise can dramatically affect the macroscopic behaviour predicted by the deterministic equations of evolution, if coupled to these equations in a multiplicative way.

All cases considered here refer to such multiplicative coupling. In this respect, our analysis differs from the work of Lemke[14] and Fraedrich[5] which is concerned primarily with additive fluctuations. Although such fluctuations are important, clearly the multiplicative coupling is a more appropriate representation of the dynamics of a complex system such as the Earth–atmosphere.

From the mathematical point of view, the effects of external noise change equation (1) to a stochastic differential equation, to which the Itô calculus can be applied[15]. Let us adopt an abstract notation and decompose equation (1) into two pieces, $f(T)$ and $g(T)$, which are linearly coupled through some parameter λ

$$\frac{dT}{dt} = f(T) + \lambda g(T) \qquad (2)$$

Let λ be subject to environmental fluctuations referred to above. For simplicity, we take the idealised picture of a gaussian white noise. (The possible shortcomings of white noise, related to the possibility that the fluctuating parameters reach negative values, means that in each case the nature of the boundaries of the stochastic process must be checked carefully.) Hence[15]:

$$\lambda = \bar{\lambda}(1 + \xi_t)$$

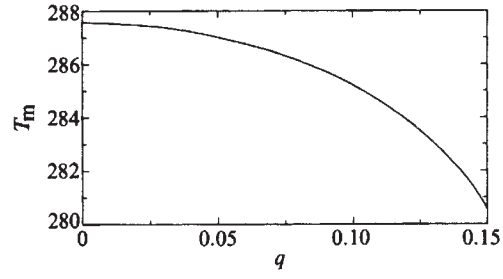

Fig. 1 Dependence of most probable temperature T_m on variance q. Q fluctuates around the mean value of 1.95 cal cm^{-2} min^{-1}. The thermal inertia coefficient used in the simulation is C = 7.5 kcal cm^{-2} K^{-1}. The emissivity ε is kept at the value 0.6, and the albedo is $a = \alpha + \beta T$ where $\alpha = 2.7888$, $\beta = -0.0086$.

0028-0836/79/370132—03$01.00

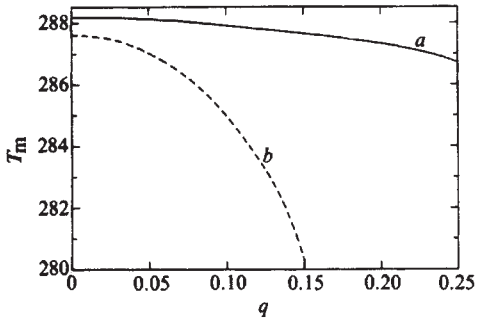

Fig. 2 T_m versus q when ε fluctuates around the value of 0.6. The thermal inertia coefficient is as in Fig. 1. *a*, The albedo is taken to be constant, $\bar{a} = 0.31$. *b*, The albedo is described by $a = \alpha + \beta T$ where $\alpha = 2.788$, $\beta = -0.0086$.

where $\bar{\lambda}$ is the value of λ appearing in the deterministic description and ξ_t is the derivative of a Wiener process, W_t:

$$\langle \xi_t \rangle = 0$$
$$\langle \xi_t \xi_{t'} \rangle = q^2 \, \delta(t - t') \tag{3}$$

Equation (2) then takes the form (we now use the Itô rather than the Stratonovich interpretation[15]):

$$dT = [f(T) + \bar{\lambda} g(T)]\, dt + q \bar{\lambda} g(T)\, dW_t \tag{4}$$

which is equivalent to a Fokker–Planck equation for the probability distribution $P(T, t)$:

$$\frac{\partial P}{\partial t} = -\frac{\partial}{\partial T}[f(T) + \bar{\lambda} g(T)]P(T, t) + \\ + \tfrac{1}{2} q^2 \frac{\partial^2}{\partial T^2} \bar{\lambda}^2 g^2(T) P(T, t) \tag{5}$$

A macroscopically observable stable temperature clearly corresponds to a maximum of the steady-state distribution $P_{st}(T)$ which obeys the equation:

$$-[f(T_m) + \bar{\lambda} g(T_m)] + \frac{q^2}{2} \frac{d}{dT}[\bar{\lambda}^2 g^2(T_m)] = 0 \tag{6}$$

we now apply this relation to the following situations.

(1) Q fluctuates around the present-day value of 1.95 cal cm^{-2} min^{-1}. If the planetary albedo, a, is taken to be constant, the noise becomes additive and equation (6) gives $dg^2/dT = 0$; hence one obtains the usual value of planetary temperature corresponding to present-day conditions. On the other hand, the fluctuations of Q begin to be effective if the planetary albedo depends on T. The simplest non-trivial such dependence is given by the linear function $a(T) = \alpha + \beta T$. Such expressions have been used widely[5,6,16], at least in the range between the highest temperature than can exist when the whole Earth is covered with ice, and the lowest possible temperature when no ice is present. Note that some pathological properties of linear albedo–temperature feedback pointed out by Schneider and Gal-Chen for one-dimensional energy-balance models[17] are not necessarily reproduced in a zero-dimensional planetary model. In the latter, the albedo must depend on the planetary temperature in a continuous fashion at least in a range of temperatures not too remote from present-day conditions.

(2) ε fluctuates around some mean value $\bar{\varepsilon}$ corresponding to a surface temperature of 287.6 K in the absence of fluctuations. The planetary albedo is taken to be, successively, equal to a constant value $\bar{a}$ or to a linear function of T. Physically speaking, fluctuations of ε at fixed albedo could be attributed to random modifications of atmospheric composition.

(3) a and ε both follow the fluctuations of cloudiness, n. The parameterisations of a and ε in terms of n are taken from Cess[16] and Schneider[18], and

$$n = 0.5(1 + \xi_t) \tag{7}$$

We now describe the results of some representative numerical simulations.

Figure 1 shows T_m as a function of q, the square root of the variance of Q. As q increases from 0.005 to 0.05 the most probable temperature decreases from about 287.6 K to 287 K. For higher q the decrease of T_m is more pronounced.

Finally, when $q \geq 0.16$ then T_m drops to extremely low values. The precise numbers are of no importance here, as the model should not be valid anyway for such ranges of temperature and additional feedback mechanisms could take over. The main point therefore of Fig. 1 is the tendency for runaway to lower temperature values.

Curve *b* of Figure 2 shows the analogous result in terms of the variance of ε for a linear albedo–temperature feedback (note that in this case equation (6) is an equation of seventh degree in T_m—a degree higher than that of the deterministic equation). Again, for $q \geq 0.16$ there is a similar tendency of runaway to extremely low values of T_m. Curve *a* describes the situation in the constant albedo case: the same tendency to lower T is observed, although there seems to be no runaway effect.

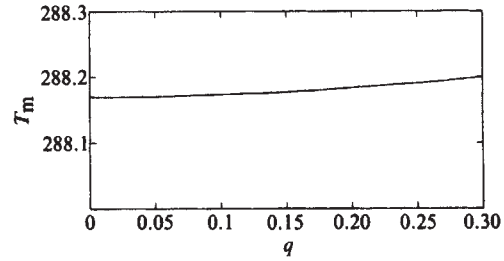

Fig. 3 Effect of fluctuating cloudiness using the following parameterisations. For the albedo (see ref. 16): $a = 0.18 + 0.26n$. For the emissivity (see ref. 18, for an effective cloud height of about 6.5 km): $\varepsilon = 0.71 - 0.22n$.

The effect of fluctuating cloudiness is rather different and described in Fig. 3 (here again, the equation for T is of seventh degree). As q increases from 0 to 0.30, the temperature remains substantially the same, varying by less than one-tenth of a degree. It appears that the fluctuations have opposite effects on the input and output terms in equation (4), thus giving a small overall effect. Another cause of the smallness of the effect may be that in the parameterisation of equation (7), cloudiness is taken to be temperature independent.

The thermal regime in a fluctuating environment seems thus to be established at temperatures that may differ substantially from those corresponding to a constant environment (actually, there always seems to be a tendency towards decreasing values). Eventually, in the presence of giant fluctuations a runaway regime may be reached in which there cannot be a stationary solution in a physically reasonable temperature range. These unexpected phenomena are all due to the multiplicative coupling between fluctuating parameters and the temperature[11]. In the case of additive noise or of linearised response[5,14] the effect would vanish because the function g^2 in equation (6) would be constant. One would thus recover the solution of the deterministic rate equation. It would be interesting to extend the present investigation to more realistic types of noise and to conditions prevailing in other planets, where a runaway regime is believed to exist.

We thank Dr W. Horstkemke for helpful discussions.

Received 6 February; accepted 20 July 1979.

1. Budyko, M. *Tellus* **21**, 611–619 (1969).
2. Sellers, W. D. *J. appl. Met.* **8**, 392–400 (1969).
3. North, G. *J. atmos. Sci.* **32**, 2033–2043 (1975).
4. Ghil, M. *J. atmos. Sci.* **33**, 3–20 (1976).
5. Fraedrich, K. *Q. Jl R. met. Soc.* **104**, 461–474 (1978).
6. Crafoord, C. & Källén, E. *J. atmos. Sci.* **35**, 1123–1125 (1978).
7. Nicolis, C. *Tellus* **31**, 193–198 (1979).
8. Dicke, R. H. *Nature* **276**, 676–680 (1978).

9. Tavakol, R. K. *Nature* **276**, 802–803 (1978).
10. Lorenz, E. N. *J. appl. Met.* **9**, 325–329 (1970).
11. Horsthemke, W. & Malek-Mansour, M. *Z. Phys.* **B24**, 307–313 (1976).
12. Arnold, L., Horsthemke, W. & Lefever, R. *Z. Phys.* **B29**, 367–373 (1978).
13. Hasselmann, K. *Tellus* **28**, 473–485 (1976).
14. Lemke, P. *Tellus* **29**, 385–392 (1977).
15. Arnold, L. *Stochastic Differential Equations* (Wiley, New York, 1973).
16. Cess, R. D. *J. atmos. Sci.* **33**, 1831–1842 (1976).
17. Schneider, S. & Gal-Chen, T. *J. geophys. Res.* **78**, 6182–6194 (1973).
18. Schneider, S. *J. atmos. Sci.* **29**, 1413–1422 (1972).

Intercalation of amino acids and polypeptides into 2H-TaS_2

V. M. Chapela* & G. S. Parry

Department of Chemical Engineering and Chemical Technology, Imperial College, London SW7, UK

2H-TaS_2 can be intercalated by organic amines and empirical rules have been formulated[1–3] governing the properties that chemical species must possess in order to intercalate. One of these rules is that molecules in which the nitrogen is basic ($pKa > 4$) usually form stable compounds provided the amine does not have bulky substituents. For certain amino acids, the values of pKa are significantly larger than this critical value (for example, glycine $pK_2 = 9.78$)[5] so that if the zwitterion is in a state where it can function as a base, it might be expected that the amino acid would intercalate 2H-TaS_2. This prediction has been verified for a number of amino acids. The discovery of these intercalation reactions provides a new range of intercalated compounds for study and also opens up the possibility of *in situ* polymerisation.

Saturated solutions of amino acids (chromatographically homogeneous or laboratory grade purity) in distilled water were prepared in a borosilicate glass ampoule at 75 °C. Samples of about 0.15 g of 2H-TaS_2, in either powder or single crystal form, were added and the ampoule was then sealed in air. The tubes were placed in an oven at 100 °C for between 1 and 3 weeks.

The intercalation reaction was monitored by opening capsules sequentially and examining the powder on an X-ray diffractometer with CuKα radiation. When the reaction product was entirely the stage 1 compound (judged by the position and line breadth of the 00l reflections), the new interlayer separation was obtained by extrapolating the parameter estimated from individual 00l reflections to $\theta = 90°$ as a function of cot θ cos θ. Selected single crystals were also examined using a single crystal goniometer with MoKα radiation.

The composition x in the formula TaS_2 (amino acid)$_x$ was determined using a Perkin-Elmer thermobalance. In making this calculation, the entire weight loss was attributed to amino acid for there was no sudden change in the rate of weight loss as might be expected if water was also intercalated along with the amino acid.

Superconducting transition temperatures were measured using a lock-in variable impedance method. Temperatures were measured using an Allen-Bradley carbon resistance thermometer calibrated against the vapour pressure of liquid helium and the superconducting transition temperatures of lead and niobium as calibration points. As noted in Table 1, certain compounds did not exhibit a superconducting transition between 1.2 and 15 K.

The intercalated species are shown in Table 1 and include amino acids such as glycine, β-alanine, L-proline, picolinic acid, diketopiperazine (glycine anhydride) as well as the polypeptides of glycine to pentaglycine. Attempts to intercalate isonicotinic acid, DL-proline and L-hydroxyproline were not successful. Values of the expanded gap (the difference between the layer separation before and after intercalation) show that, except for valine, the molecules lie parallel to the TaS_2 layer with the p_z orbital containing the nitrogen lone pair orientated perpendicular to the layer. The results indicate that the peptide bond actively promotes intercalation. Thus glycine anhydride does not possess any amino groups at all and intercalation must have involved the two ring nitrogen atoms. Moreover pentaglycine (a 16-atom chain excluding hydrogens) remains parallel to the layer with an expanded gap of 3.4 Å in contrast to pentadecylamine[1] (also a 16-atom chain) which lies perpendicular to the layer with a 39 Å expanded gap.

Single-crystal X-ray studies indicate that the a-axis orientation of the matrix crystal is preserved on intercalation although the layer stacking order is destroyed (only hk rods are observed). This suggests a random sequence of stacking faults in contrast to the regular sequence of faults found in 2H-TaS_2(pyridine)[4]. Possibly the present choice of reaction conditions does not favour a highly orientated reaction product.

* Permanent address: Centro de Investigacion de Materiales, UNAM, Apartado Postal 70–360, Cuidad Universiaria, Mexico 20, D.F., Mexico.

Table 1 Amino acids and polypeptides intercalating with 2H-TaS_2

Formula	Substance	pK_2*	Aq. conc. (g ml^{-1})†	x‡	Interlayer § separation (Å)		Expanded gap (Å)¶	Superconductivity: T onset (K)	Superconductivity: Width (K)
$NH_2.CH_2COOH$	Glycine	9.78	0.25	0.289	9.71	(0.009)	3.67	3.4	1.1
$NH_2.(CH_2.CO.NH)_{n-1}.CH_2.COOH$	Diglycine $n = 2$	8.25	0.125	0.172	9.43	(0.016)	3.39	2.6	0.6
	Triglycine $n = 3$	8.09	0.125	0.085	9.40	(0.017)	3.36	4.2	1.4
	Tetraglycine $n = 4$		0.036	0.076	9.4	(0.04)	3.4	No transition detected	
	Pentaglycine $n = 5$		0.005	0.066	9.4	(0.04)	3.4	between 1.2 and 1.5 K	
$CO.NH.CH_2.CO.NH.CH_2$	Glycine anhydride (dikentopiperazine)		0.080	0.158	9.5	(0.05)	3.5	2.8	0.8
$CH.CH.CH.CH.N.C.COOH$	Picolinic acid		0.200	0.163	9.4	(0.03)	3.4	3.4	1.4
$CH.CH.CH.N.CH.C.COOH$	Nicotinic acid		0.166	0.165	9.56	(0.005)	3.52	3.6	1.8
$CH(CH_2)_2.CH(NH_2).COOH$	Valine	9.72	0.100	0.255	12.6	(0.07)	6.6	No transition detected between 1.2 and 15 K	
$NH_2.CH_2.CH_2.COOH$	β-Alanine		0.050	0.219	9.4	(0.04)	3.4	2.5	0.5
$CH_2.CH_2.CH_2.NH.CH.COOH$	L-Proline		0.400	0.181	10.00	(0.014)	3.96	4.7	2.7

* From ref. 5.
† Aqueous concentration: this solution was allowed to react for 7 days at 95 °C.
‡ Composition TaS_2(amino acid)$_x$.
§ The e.s.d. is given in parenthesis.
¶ The difference between the interlayer separation before and after intercalation.

0028–0836/79/370134—02$01.00